DOI: 10.1002/cmdc.201402315

3-Deazaneplanocin A and Neplanocin A Analogues and Their Effects on Apoptotic Cell Death

Eric K. W. Tam,[a] Tuan Minh Nguyen,[a] Cheryl Z. H. Lim,[b] Puay Leng Lee,[b] Zhimei Li,[b] Xia Jiang,[b] Sridhar Santhanakrishnan,[a] Tiong Wei Tan,[a] Yi Ling Goh,[a] Sze Yue Wong,[a] Haiyan Yang,[a] Esther H. Q. Ong,[c] Jeffrey Hill,[c] Qiang Yu,*[b] and Christina L. L. Chai*[a, d]

3-Deazaneplanocin A (DzNep) is a potential epigenetic drug for the treatment of various cancers. DzNep has been reported to deplete histone methylations, including oncogenic EZH2 complex, giving rise to epigenetic modifications that reactivate many silenced tumor suppressors in cancer cells. Despite its promise as an anticancer drug, little is known about the structure–activity relationships of DzNep in the context of epigenetic modifications and apoptosis induction. In this study, a number of analogues of DzNep were examined for DzNep-like ability to induce synergistic apoptosis in cancer cells in combination with trichostatin A, a known histone deacetylase (HDAC) inhibitor. The structure–activity relationship data thus obtained provide valuable information on the structural requirements for biological activity. The studies identified three compounds that show similar activities to DzNep. Two of these compounds show good pharmacokinetics and safety profiles. Attempts to correlate the observed synergistic apoptotic activities with measured *S*-adenosylhomocysteine hydrolase (SAHH) inhibitory activities suggest that the apoptotic activity of DzNep might not be directly due to its inhibition of SAHH.

1. Introduction

Epigenetic alterations play important roles in cancer development. These alterations, including DNA hypermethylation and chromatin modifications such as histone methylation and deacetylation,[1] have provided new targets for therapeutic interventions in cancer cells. While advancements have been made in the last decade in the development of inhibitors targeting histone deacetylation or DNA methylation for cancer therapy,[2] there is little progress in the development of histone methylation inhibitors. Aberrant histone methylation, such as histone H3 lysine trimethylation (H3K27me3) induced by oncogenic polycomb protein histone methyltransferase EZH2, has been frequently linked to tumorigenesis,[3] so there has been tremendous effort directed towards the development of small molecules that target EZH2.

We previously reported 3-deazaneplanocin A (DzNep) (Figure 1), an *S*-adenosylhomocysteine (AdoHcy) hydrolase (SAHH) inhibitor that can effectively deplete cellular levels of the EZH2 complex, inhibit H3K27me3 and other histone methylations, and induce apoptosis in cancer cells, but not in normal cells, through the reactivation of many silenced tumor suppressors in cancer cells.[4] Although this compound does not appear to be specific for EZH2–H3K27me3, its anticancer activity associated with the depletion of EZH2 has been demonstrated in vitro and in vivo in many cancer types, including breast, lung, liver, prostate, leukemia.[5] Recent efforts have led to the discovery of a number of selective EZH2 inhibitors, for example, EPZ005687,[6] GSK126,[7] and EI1.[8] However, these inhibitors seem to have anticancer activity only in B cell lymphomas that carry activating mutations of EZH2, but not in epithelial tumors in which enhanced EZH2 activity is mainly caused

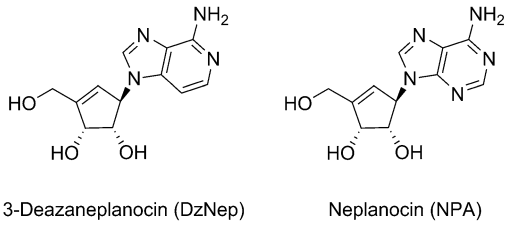

3-Deazaneplanocin (DzNep) Neplanocin (NPA)

Figure 1. Structures of 3-deazaneplanocin A (DzNep) and neplanocin (NPA).

[a] *Dr. E. K. W. Tam, Dr. T. M. Nguyen, Dr. S. Santhanakrishnan, T. W. Tan, Y. L. Goh, S. Y. Wong, H. Yang, Prof. C. L. L. Chai*
Institute of Chemical & Engineering Sciences
*Agency for Science, Technology & Research (A*STAR)*
8 Biomedical Grove, Neuros #07-01, Singapore 138665 (Singapore)
E-mail: christina_chai@ices.a-star.edu.sg

[b] *C. Z. H. Lim, P. L. Lee, Z. Li, X. Jiang, Dr. Q. Yu*
Cancer Therapeutics & Stratified Oncology, Genome Institute of Singapore
*Agency for Science, Technology and Research (A*STAR)*
60 Biopolis Street, #02-01, Singapore 138672 (Singapore)
E-mail: yuq@gis.a-star.edu.sg

[c] *E. H. Q. Ong, Dr. J. Hill*
Experimental Therapeutics Centre
*Agency for Science, Technology and Research (A*STAR)*
31 Biopolis Way, Nanos Level 3, Singapore 138669 (Singapore)

[d] *Prof. C. L. L. Chai*
Department of Pharmacy, National University of Singapore
18 Science Drive 4, Singapore 117543 (Singapore)
E-mail: phacllc@nus.edu.sg

Supporting information for this article is available on the WWW under http://dx.doi.org/10.1002/cmdc.201402315.

by increased gene expression. Intriguingly, a recent study showed that although inhibitors of EZH2, such as GSK126, have robust activity in the depletion of H3K27me3 in epithelial tumors cells, they have little effect on cancer cell growth.[9] Moreover, a peptide that induces the depletion of EZH2 protein complex is sufficient to inhibit cell growth.[10] This raises a possibility that targeting the EZH2 complex, rather than inhibiting H3K27me3, is required for blocking the EZH2-mediated oncogenic effect. Given the remarkable activities of DzNep in the depletion of EZH2 and in the inhibition of tumor growth, we were intrigued with the possibilities of examining DzNep derivatives so as to obtain a better understanding of the structure–activity relationships.

In this study, we report a comprehensive cell-based structure–activity relationship study where we screened for DzNep-like activities for the induction of apoptosis in cancer cells. We also report the IC_{50} values of selected DzNep analogues against human SAHH enzymes with the objective of determining if a correlation exists between SAHH inhibition and the ability of the compounds to induce apoptosis.

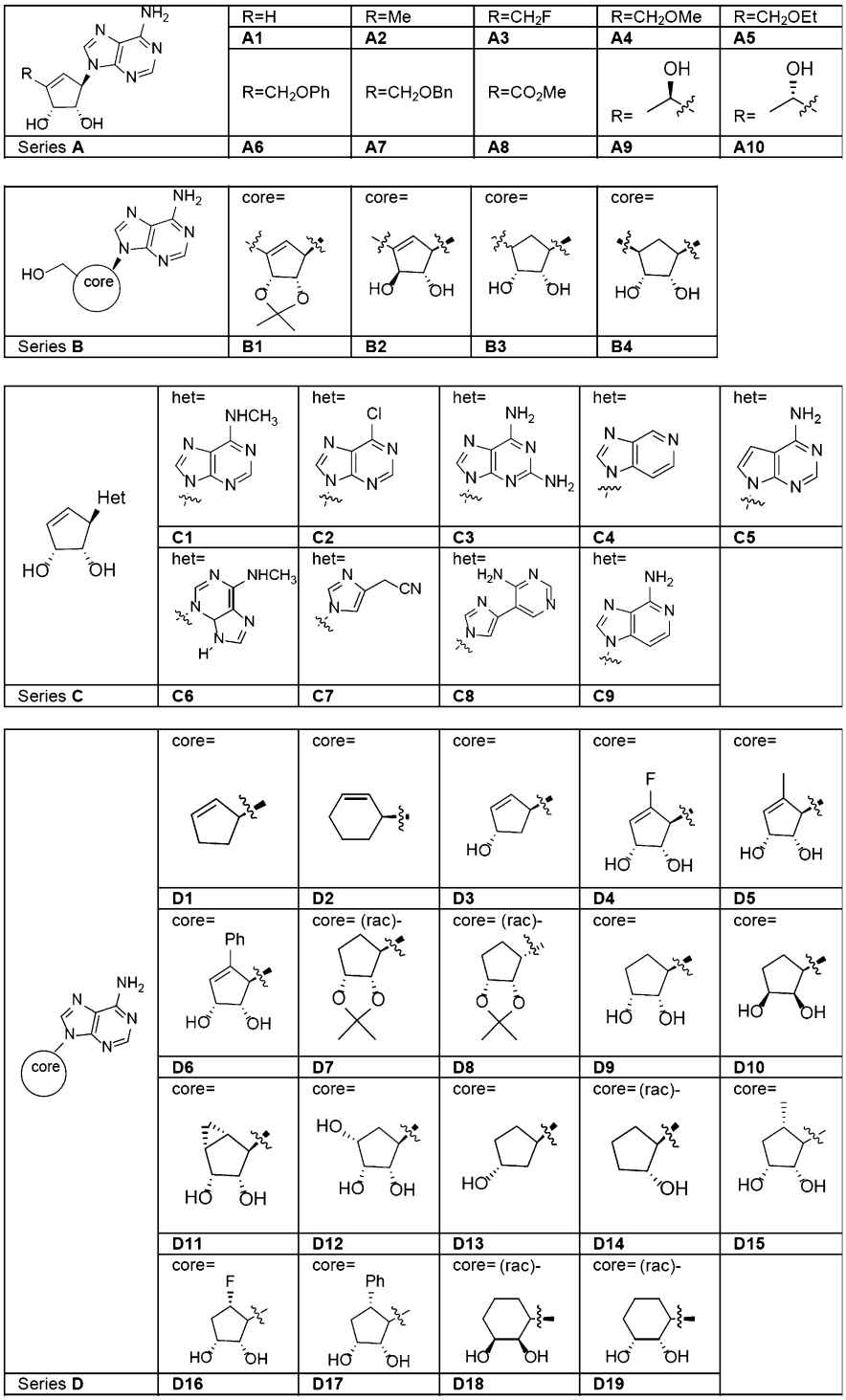

Figure 2. Compounds used for structure–activity determination. Series **A** includes variations in substituents attached to the carbocyclic ring system of NPA. Series **B** and **D** include variations in the carbocyclic ring system. Series **C** includes variations in the heterocyclic ring attached. For **D7**, **D8**, **D14**, **D18**, and **D19**, the relative stereochemistry is shown.

2. Results

2.1 Synthesis of the target compounds

Our early studies have shown that the natural product, neplanocin A (NPA) (Figure 1) is able to induce the same level of apoptosis as DzNep in cellular models (unpublished observations). We thus designed and synthesized a total of 40 compounds based on variations in the structure of DzNep and NPA (Figure 2). They include 1) variations in the substituents attached to the carbocyclic ring system of NPA (series **A**, compounds **A1**–**A10**), 2) variations in the carbocyclic ring system (series **B** and **D**, compounds **B1**–**B4**, **D1**–**D19**), 3) variations in the nature of the heterocyclic ring attached to the carbocyclic ring (series **C**, compounds **C1**–**C9**). Only the synthesis of selected compounds is discussed here. The full experimental details on the synthesis of the target compounds can be found in the Supporting Information.

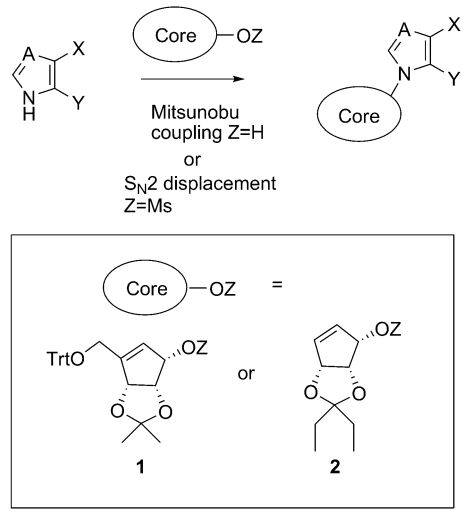

Scheme 1. Key coupling step to target compounds.

In general, the target compounds were synthesized by reacting the carbocyclic scaffold ("core") with the appropriate heterocyclic bases under Mitsunobu or S_N2 conditions (Scheme 1). For compounds in series **A** and **C**, the core is comprised of functionalized cyclopentene **1** and **2**, while the compounds in series **B** and **D** were either commercially available or were synthesized following literature procedures (see Supporting Information).

Cyclopentenol **1** ($Z = H$) was synthesized in eight steps starting from D-ribose,[11] and subsequent transformations gave protected NPA **3** in good yields. With the protected NPA in hand, protected precursors of **A2–A10** were accessed from this advanced intermediate as summarized in Scheme 2. Compound **4** was directly accessed from **3** through the reaction of the alcohol with 1,1′-thiocarbonyl diimidazole and tributyltin hydride, while the synthesis of **5** was achieved using dimethylaminosulfur trifluoride (DAST). Methylation, ethylation, and benzylation of **3** gave the *O*-analogues **6**, **7,** and **9**, respectively. Phenoxy derivative **8** was obtained under Mitsunobu conditions, while methyl ester **10** was accessed via a three-step pro-

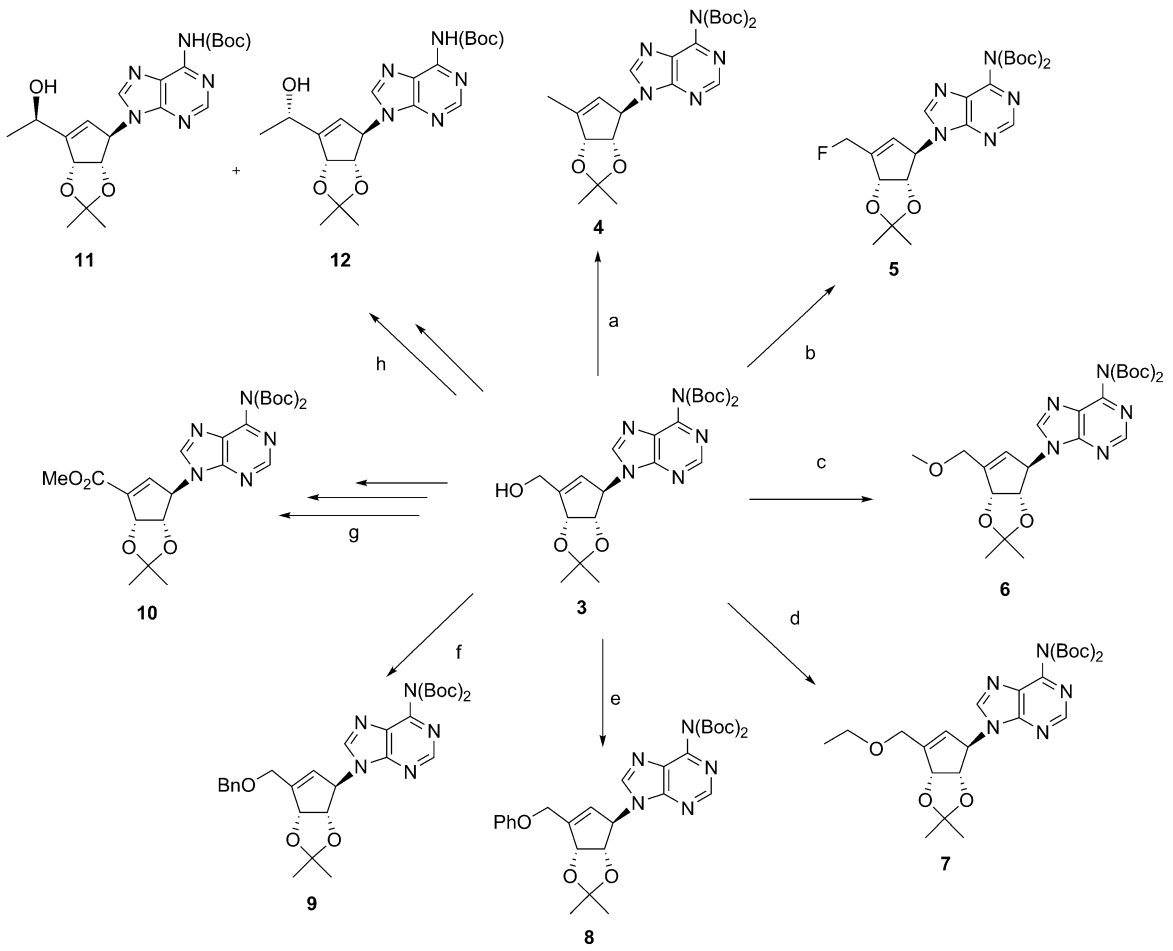

Scheme 2. *Reagents and conditions*: a) 1. 1,1′-thiocarbonyl diimidazole, RT, 18 h, CH_2Cl_2, 56%, 2. tributyltinhydride, 110 °C, 8h, 56%; b) DAST, RT, 3 h, 72%; c) MeI, NaH, DMF, RT, 16 h, 54%; d) EtI, NaH, DMF, RT, 16 h, 25%; e) PhOH, PPh_3, DIAD, THF, RT, 18 h, 78%; f) BnBr, NaH, DMF, RT, 16 h, 39%; g) 1. Dess–Martin periodinane, CH_2Cl_2, RT, 17 h, 95%, 2. oxone, DMF, RT, 48 h, 74%, 3. (trimethylsilyl)diazomethane, MeOH/toluene (2:3), RT, 48 h, 47%; h) 11. Dess–Martin periodinane, CH_2Cl_2, RT, 17 h, 95%; 2) MeMgBr, THF, 0 °C→RT, 16 h, 86%.

cedure (oxidation to the aldehyde with Dess–Martin periodinane, followed by oxidation to the acid and esterification) from alcohol **3**. Compounds **11** and **12** were derived from the same aldehyde by treatment with methyl magnesium iodide. In all cases, global deprotection of the *tert*-butyloxycarbonyl (Boc) and acetonide protecting groups under acidic conditions afforded the target compounds.

For the synthesis of cyclopentenol **15**, D-ribose was converted, through a sequence of reactions, to a diastereomeric mixture of dienes **13** following modified procedures (Scheme 3).[12]

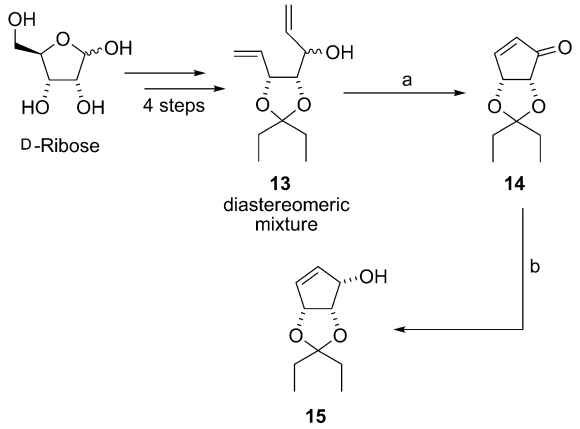

Scheme 3. *Reagents and conditions*: a) 1. 2nd-gen. Hoveyda–Grubbs catalyst, CH_2Cl_2, RT, 4 h, 2. pyridinium chlorochromate, Celite, CH_2Cl_2, RT, 4 h (Overall yield of 55% from the aldehyde; see Supporting Information for details); b) $NaBH_4$, $CeCl_3$, 0 °C→RT 85–95%.

Ring-closing metathesis followed by pyridinium chlorochromate (PCC) oxidation gave enone **14** in reasonable yields. The ketone functionality of the enone was then reduced under Luche's conditions to afford a single stereoisomer (**15**) in high isolated yields. With this alcohol **15** in hand, coupling with *N*,*N*-diprotected adenine followed by deprotection gave compound **A1** in good yields (Scheme 4). Subsequent hydrogenation of **A1** gave compound **D9** in quantitative yields.

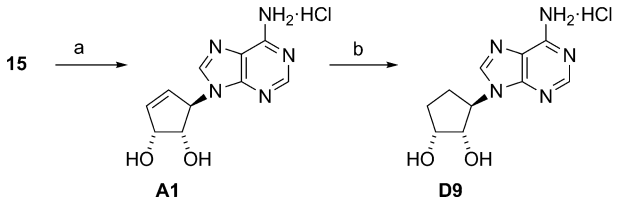

Scheme 4. *Reagents and conditions*: a) 1. PPh_3, DIAD, diBoc adenine, THF, 80%, 2. 10% HCl in H_2O/MeOH (1:1), 90%; b) H_2, 10% Pd/C, H_2O, RT, 24 h, 95%.

The synthesis of **D4** and **D16** are summarized in Scheme 5. Using enone **14** as described in Scheme 4, iodination followed by reduction of ketone **16** provided alcohol **17** in good yields. The free hydroxy group of **17** was protected as its *tert*-butyldiphenylsilyl (TBDPS) ether **18**. Fluorination of iodo-alkene **18** with excess *N*-fluorobenzenesulfonimide (NFSI) and BuLi furnished an inseparable mixture of compounds **19** and **20** in a ratio of 3:1, which was used as is in the subsequent steps. Deprotection of the TBDPS groups of the mixture of **19** and **20**

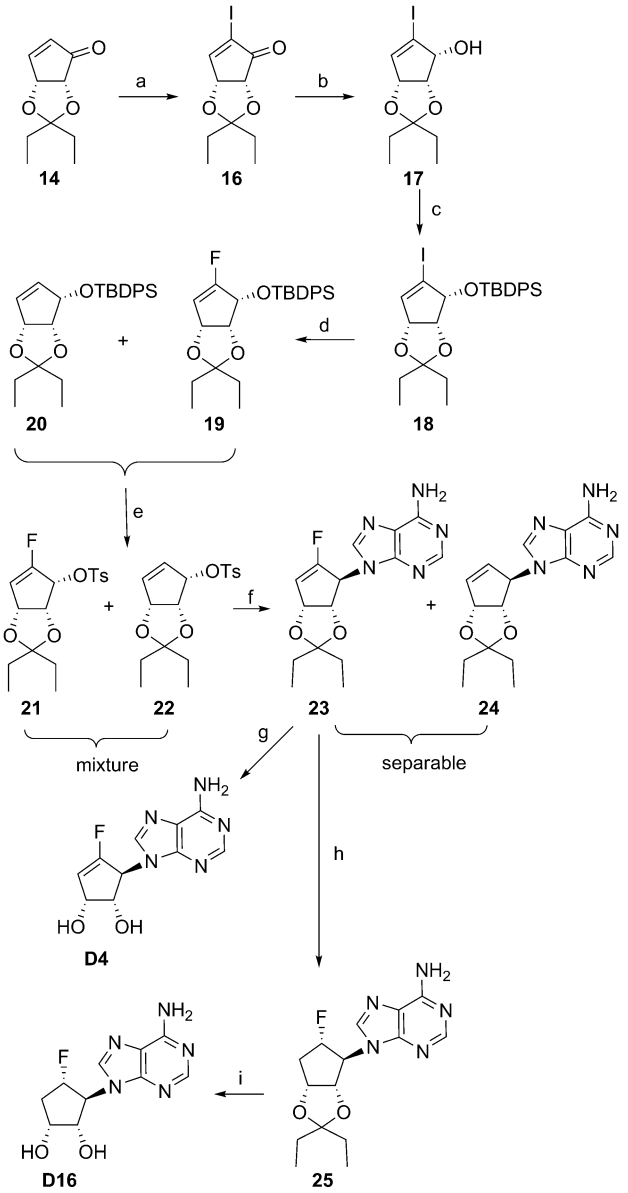

Scheme 5. *Reagents and conditions*: a) I_2, pyridine, CH_2Cl_2/THF (10:1), RT, 18 h, 75%; b) $NaBH_4$, $CeCl_3$, MeOH, 0 °C→RT, 1 h, 98%; c) TBDPSCl, imidazole, CH_2Cl_2/THF (10:1), RT, 18 h, 93%; d) *n*BuLi, NFSI, THF, −60 °C, 4 h; e) 1. TBAF, THF, RT, 18 h, 2. TsCl, Et_3N, DMAP, CH_2Cl_2, RT, 18 h; f) adenine, NaH, DMF, 80 °C, 18 h, 28% over four steps for **23**; g) 2 N HCl, RT, 48 h, 79%; h) 10% Pd/C, H_2 (50 psi), MeOH, RT, 16 h, 73%; i) 2 N HCl, RT, 48 h, 95%.

using tetrabutylammonium fluoride (TBAF) provided an inseparable mixture of alcohols. Tosylation of the mixture to give **21** and **22**, followed by alkylation with adenine in *N*,*N*-dimethylformamide (DMF), yielded a mixture of **23** and **24**, which was separable by column chromatography. The reduction of the double bond of **23** in the presence of Pd/C under high pressure (50 psi) provided **25** in 73% yield. The stereochemistry of the fluorine substituent and the basic skeleton of **25** was unambiguously characterized by X-ray crystallography (see Supporting Information). Hydrolysis of **25** in acidic medium gave **D16** in good yields. Similarly, hydrolysis of **23** furnished **D4** in good yields.

Compounds **D5**, **D6**, **D15,** and **D17** were synthesized from versatile iodocyclopentenes **17** and **18** through palladium-catalyzed reactions followed by a sequence of transformations similar to that described previously (Scheme 6; see Supporting Information for details). The stereochemistry of the vicinal hydroxy groups of the cyclopentane ring in compounds **D15** and **D17** is presumed to be *syn*, based on observation made with **D16**.

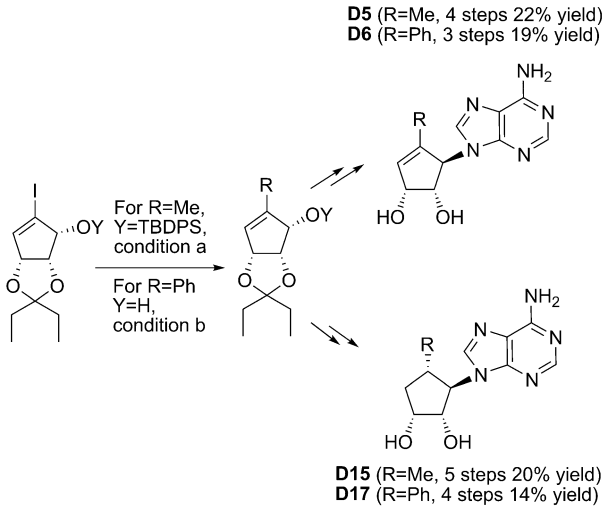

Scheme 6. Synthetic routes to **D5**, **D6**, **D15,** and **D17**. *Reagents and conditions*: a) $PdCl_2(PPh_3)_2$, $AlMe_3$, THF, 50 °C, 18 h; b) Phenylboronic acid, $PdCl_2(PPh_3)_2$, Na_2CO_3, toluene/MeOH, 50 °C, 18 h. (See Supporting Information for details).

2.2 Cell-based structure–activity relationship studies

We have previously shown that DzNep is able to synergize with histone deacetylase (HDAC) inhibitor, trichostatin A (TSA), to potently induce apoptosis in colon cancer DLD1 cells.[13] We also showed that DzNep potently induces apoptosis upon activation of transcription factor E2F1 in colon cancer cell HCT116.[14] We thus used these two independent in vitro cellular systems to determine the cellular activities of the DzNep-like compounds described here. Initially, DLD1 cells were used to screen for DzNep analogues that can increase apoptosis in combination with TSA. DLD1 cells were treated with DzNep analogues (5 μM) for 48 h followed by the HDAC inhibitor TSA (150 nM) for an additional 24 h before harvesting for apoptosis assessment using fluorescent-activated cell sorting (FACS) analysis of DNA content. The positive hits were compounds that show increased apoptotic cell death on drug combination, that is to say, where the apoptotic cell death is greater than the sum of that caused by treatment with the DzNep analogue or TSA alone. The results are summarized in the Supporting Information.

From the screening studies, the effect of substitution (R) at the C-4 position of the carbocyclic ring of NPA was investigated. Positive hits are compounds **A1**–**A4**, **A9,** and **A10** (i.e., compounds possessing H, Me, CH_2F, CH_2OMe, $CH(OH)CH_3$ substituents instead of the CH_2OH substituent present in NPA). Replacement of the carbocyclic ring of NPA with other carbocyclic core structures (series **B**) indicated that the free hydroxy substituents are critical for DzNep-like apoptotic activity as is the stereochemistry of the hydroxy groups, as **B1** and **B2** do not show any synergistic activity. Surprisingly, saturation of the double bond (cyclopentane vs cyclopentene; **B3**) retained the synergistic apoptotic activity.

In view of the simplicity of the structure of **A1**, further structural modifications were centered on variations of this derivative. Compounds in series **C** examined the effect of varying the heterocyclic bases, and none of the compounds tested in this series show any significant DzNep-like apoptotic activity. Series **D** further examined the effect of varying the carbocyclic core. Consistent with the observations made previously, saturation of the double bond of **A1** (**D9**) retained the apoptotic activity. The vinyl fluoride derivative **D4** and the saturated compound **D16** showed synergistic apoptotic cell death, while all other variations of the carbocyclic core resulted in loss of apoptotic activity. This indicates the sensitivity of the carbocyclic core in inducing apoptosis. As observed with compounds in series **B**, the location, stereochemistry, and presence of both the secondary hydroxy groups are critical for apoptosis. In addition, the ring size is also important. From these studies, three compounds **D4**, **D9**, and **D16** have been identified as showing synergistic apoptotic activity comparable with DzNep.

A secondary screen with selected positive hits was carried out with HCT116 cells in which E2F1 is fused to the 4-hydroxytamoxifen (4-OHT)-responsive ligand-binding domain of the estrogen receptor (ER) to form an ER–E2F1 fusion protein, which becomes activated after addition of 4-OHT. We have previously shown that DzNep, upon addition of 4-OHT (to activate E2F1) in cell culture, potently induced apoptosis in this system, while only a modest level of apoptosis was induced in the absence of 4-OHT.[14]

As shown in Figure 3, in HCT116 ER-E2F1 cells, 4-OHT and DzNep alone induced approximately 13% and 20% of cells in apoptosis, respectively, as determined by counting cells in sub-G1 phase using FACS analysis, while the combination of 4-OHT and DZNep resulted in 54% of cells in apoptosis. Compounds **A4**, **D4**, **D9**, and **D16** exhibited comparable activities to DzNep, resulting in synergistic apoptosis of 45%, 47%, 49%, and 47%,

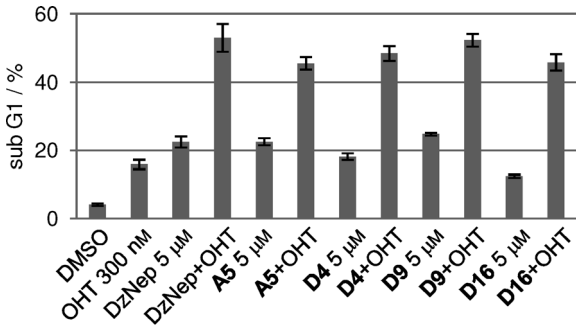

Figure 3. In vitro assessment of DzNep analogues. p53-null HCT116-ER–E2F1-expressing cells were treated with DzNep (5 μM) or DzNep analogues **A4**, **D4**, **D9** or **D16** in the presence or absence of 4-OHT (300 nM). After 72 h, cells were harvested, and cell death was assessed by propidium iodide staining using fluorescent-activated cell sorting (FACS).

respectively, when combined with 4-OHT. We also showed that the DzNep analogues have the capacity to deplete histone methylations including H3K27me3, H3K4me3, and H3K20me3, though **D9** seems to be more selective on H3K27me3 as shown in Figure 4.

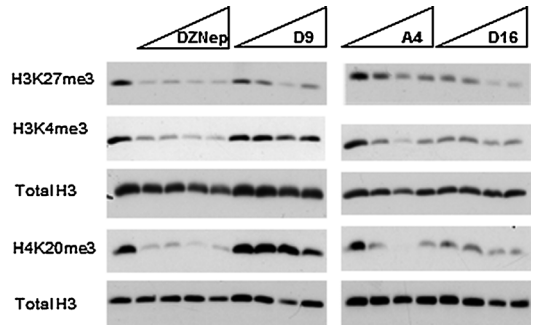

Figure 4. Western blot showing the effect of DzNep analogues on histone methylation. HCT116 cells were treated with increasing concentrations of indicated compounds (0.5, 1, 2.5 and 5 μM) for 72 h before being harvested for Western blot analysis.

2.3 SAHH inhibition by selected compounds

A total of 16 compounds (DzNep, NPA, **A1**, **A3**–**A6**, **A9**–**10**, **D4**–**6**, **D9**, **D15**–**17**) were tested for inhibition of human SAHH using an in vitro SAHH activity assay. Although the IC_{50} or K_i values of some of these compounds have already been reported in the literature, comparison of the literature values proved to be difficult due to the different assay platforms and the species and form of SAHH used (recombinant or purified native). A summary of the results is shown in Table 1. From these studies, it is noted that NPA and DzNep are potent inhibitors of SAHH, while **D9** is approximately sixfold less potent than DzNep. Interestingly **D16** was 18 fold less potent than **D9**, while the activity of **D4** and **D16** are similar. The ranking of the compounds in terms of the IC_{50} values with SAHH inhibition is NPA (most potent) > **A3** > DzNep > **D9** > **A9**–**A4** > **A10** > **A6** > **A5** > **D17** > **D16** ≈ **D4** ≈ **D15** > **A1** > **D5** ≈ **D6** (least potent).

2.4 In vitro ADME and hERG studies

Compounds **D9** and **D16** were selected for in vitro ADME evaluation and hERG studies. Measurement of the log*D* showed that both compounds have comparable values (−1.6 at pH 3.0 and −0.5 at pH 7.4). In addition, the solubility of the compounds at pH 2 and 6.5 did not change and is approximately 300 μM for both **D9** and **D16**. The half-lives of **D9** and **D16** with human liver microsomes were measured to be 2636 min and 1029 min, respectively, while that with male rat liver microsomes and male mouse liver microsomes were 183 min and 307 min for **D9** and 836 and 982 min for **D16**, respectively.

hERG safety studies were performed, and the IC_{50} values of both **D9** and **D16** were found to be greater than 100 μM using a FluxOR hERG fluorescence assay, and greater than 10 μM using the electrophysiological hERG test. From these data, it can be concluded that neither **D9** and **D16** show any significant inhibition of the hERG channel.

2.5. Antitumor effects of D9 in a xenograft tumor mouse model

To evaluate the anticancer effect of **D9** in vivo, an HCT116 subcutaneous xenograft tumor mouse model was used. In this model, 5×10^6 HCT116 cells were injected into Balb/c nude mice subcutaneously (s.c.), and when the tumors reached an average of 200 mm^3 in size, **D9** was administered through intraperitoneal (i.p.) injection. As shown in Figure 5a **D9** administration at 30 or 80 mg kg^{-1} five days a week for two weeks resulted in marked decrease in tumor growth in a dose-dependent manner. During the course of drug treatments, the body weight of mice was monitored daily. **D9** did not give rise to obvious signs of toxicity, and only a minimum loss of body weight was observed (Figure 5b). These data suggest that **D9** has significant antitumor effects while at the effective doses it

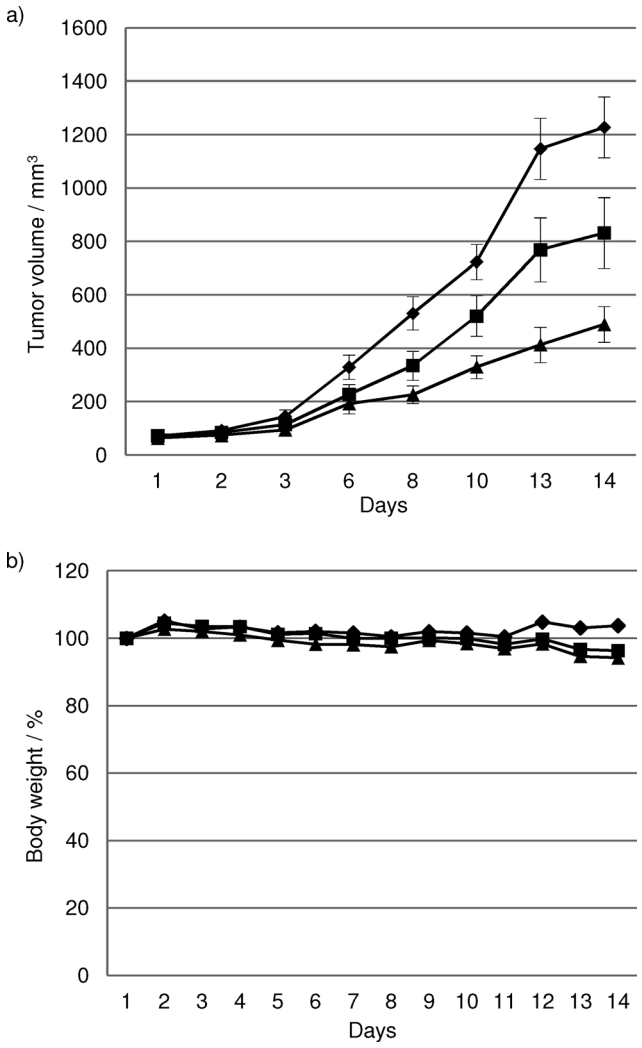

Figure 5. Effects of **D9** in vivo on a) HCT116 xenograft tumor growth and b) body weight change of mice. Group I: 10% DMSO (◆); Group II: **D9** 30 mg kg^{-1} (■); Group III: **D9** 80 mg kg^{-1} (▲).

Table 1. Inhibition (IC_{50}) of human *S*-adenosylhomocysteine hydrolase (SAHH) by DzNep derivatives.[a]

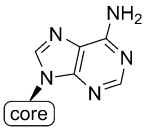

Structure		IC_{50} [μM]	Structure		IC_{50} [μM]
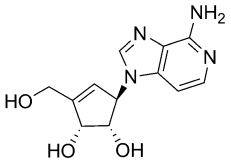	DzNep	0.23 ± 0.07 [Lit: K_i=23 nM, human SAHH][25]	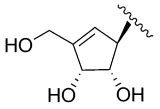	NPA	0.04 ± 0.01 [Lit: IC_{50} = 0.82 μM, human SAHH][26]
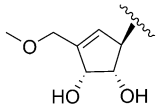	**A4**	2.22 ± 0.24 [Lit: IC_{50} > 10 μg mL^{-1}, rabbit erythrocyte][19]	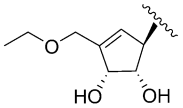	**A5**	13.1[b]
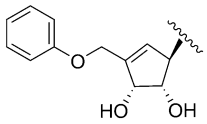	**A6**	7.47 ± 4.30	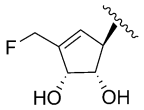	**A3**	0.13 ± 0.04 [Lit: IC_{50} > 10 μg mL^{-1}, rabbit erythrocyte][19]
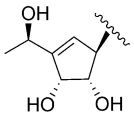	**A9**	1.71 ± 0.24 [Lit: IC_{50} = 0.2 μg mL^{-1}, rabbit erythrocyte][19]		**A9/A10** (15:85)[c]	3.46 ± 0.87
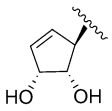	**A1**	44.59 ± 13.34 [Lit: K_i=35 nM, bovine liver][27]	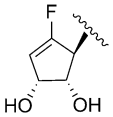	**D4**	24.39 ± 0.40
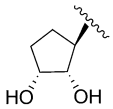	**D9**	1.35 ± 0.35 [Lit: IC_{50} = 9 μM, human SAHH][28]	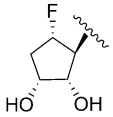	**D16**	25.18 ± 2.17
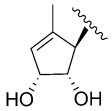	**D5**	> 200	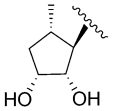	**D15**	25.7[b]
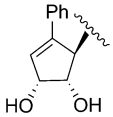	**D6**	> 200	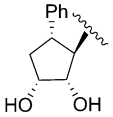	**D17**	20.9[b]

[a] Inhibition was determination using an enzyme assay with recombinant expressed human SAHH; data represent the mean ± SD of n = 2 independent experiments, unless specified otherwise. [b] Data from a single independent assay. [c] Tested as a mixture of compounds.

is well tolerated in the recipient mice (Figure 5). The pharmacokinetic profile of **D9** in Sprague–Dawley rats through oral (p.o.) administration (5 mg kg^{-1}) also suggested that **D9** is readily absorbed and has a half-life of 5 h.

3. Discussion

Our studies above have delineated some of the critical structural features required for DzNep-like apoptotic activity (Figure 6). In brief, the structure–activity relationship study identified that the 2,3-dihydroxycarbocyclic core of DzNep, whether saturated or unsaturated, is needed for synergistic activity (Figure 6). The heterocyclic base at the C-1 position of

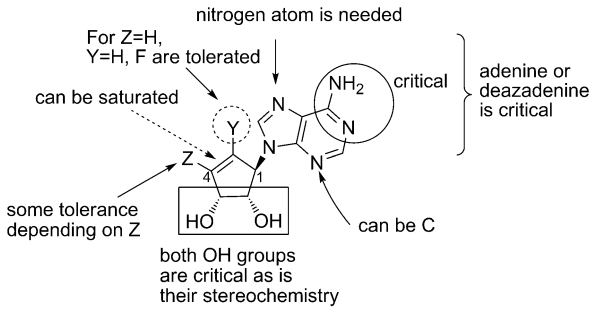

Figure 6. Critical structural features for DzNep-like apoptotic activity.

the carbocycle can either be adenine or deazaadenine, but all the other heterocyclic combinations led to loss in activity. Thus compound **A1** and **D9** contain the minimum pharmacophore required for synergistic apoptotic activity. When considering the structure–activity relationships of DzNep and NPA, it is apparent that variation in the substituents at the C-4 position cannot be easily rationalized. The presence of a substituent is not necessary for synergistic apoptotic activity, as seen with compound **A1**. There is also some tolerance for small substituents at the C-4 position of the carbocyclic ring. Interestingly, a secondary alcohol at the C-4 position does not lead to large losses in biological activity. The presence of substituents at the C-5 position of the carbocyclic ring causes large losses in synergistic apoptotic activity—the exception is when a fluorine atom replaces the hydrogen atom at C-5 of **A1** and **D9**.

SAHH is an important enzyme that catalyzes the hydrolysis of *S*-adenosylhomocysteine (AdoHcy) to adenosine and L-homocysteine.[15] Accumulation of AdoHcy through inhibition of SAHH can, in turn, lead to inhibition of methyltransferases and thus indirectly affect the epigenetic mechanisms of a cell. DzNep and NPA have long been recognized as potent inhibitors of SAHH. Indeed, early studies have focused on the development of these and related compounds as antivirals through the inhibition of SAHH.[16] The mechanisms of SAHH inhibition are suggested to occur either via a reversible Type I mechanism through the oxidation of the cofactor NAD^+ to NADH, or via an irreversible Type II mechanism of covalent binding to the active site by an inhibitor with a nucleophilic residue.[17] Of the selection of the target compounds measured for SAHH activity, the most potent SAHH inhibitor was NPA ($IC_{50}=40$ nM), followed by the fluorinated compound **A3** ($IC_{50}=130$ nM), then DzNep ($IC_{50}=230$ nM). We note that these values for NPA and DzNep differ from those reported in the literature for human SAHH.[16b,18] The compounds that were tested from series **A** showed that SAHH inhibition is sensitive to modifications of the substituents at the C-4 position. The stereoisomers of the secondary alcohol **A9** showed a 1.5-fold difference in SAHH activities as compared with the enriched mixture of **A10** (containing 15% **A9**). From the literature, a large difference in SAHH activities between **A9** and **A10** was reported, in favor of **A9**, as measured with rabbit SAHH.[19] For the selected compounds studied in series **D**, the most potent compound is **D9** which showed very different activity in comparison with the unsaturated compound **A1**. The vinyl fluoride **D4** was the best compound amongst the unsaturated compounds in series **D**, and **D4** has been reported to inhibit SAHH via the Type II mechanism.[20] The saturated compounds **D15**–**D17** have comparable SAHH activity.

Our SAHH studies identified NPA, DzNep, methyl ether **A4**, fluorinated derivative **A3**, alcohol **A9**, and **D9** as the best inhibitors of SAHH. Broadly speaking, these compounds are also potent inducers of apoptosis. However there is no discernible direct relationship between SAHH inhibition and synergistic apoptotic activities. Specifically compounds that have reasonable SAHH inhibitory activities (e.g., **D15**) do not display synergistic apoptotic activity.

4. Conclusions

The toxicities and the short half-lives of DzNep and NPA have long been known, and this is in part due to the rapid phosphorylation by adenosine kinase.[20] Through these studies, we have identified two compounds (**D9** and **D16**) that have longer half-lives than NPA and DzNep. In addition, animal studies with **D9** show that it has lower toxicity than DzNep and is effective at shrinking tumors. Thus, we have successfully identified at least two compounds, which are potentially superior to DzNep and NPA, for further development as chemotherapeutics for epigenetic therapy. Future mechanistic studies will undoubtedly shed more information on the mode of action of these compounds.

Experimental Section

Chemistry

Unless otherwise specified, materials were purchased from commercial suppliers and used without further purification. Solvents for reactions were taken from a Glass Contour solvent purification system under nitrogen. ^{1}H NMR and ^{13}C NMR spectra were acquired on a Bruker 400. UltraShield spectrometer operating at 400 MHz and 100 MHz, respectively, unless specified otherwise. Chemical shifts (δ) are given in ppm relative to respective residual solvent peaks (CD_3OD: $\delta=3.31$ ppm; [D_6]DMSO: $\delta=2.50$ ppm; D_2O: $\delta=4.79$ ppm) except for those recorded in $CDCl_3$, which were referenced to tetramethylsilane (TMS) or residual solvent peak at $\delta=7.26$ ppm. For ^{13}C NMR spectra, chemical shifts are given relative to the respective residual solvent peak (CD_3OD: $\delta=49.0$ ppm; [D_6]DMSO: $\delta=39.5$ ppm; $CDCl_3$: $\delta=77.2$ ppm). Where necessary, the signals of novel compounds were assigned by 1D NOE differences and/or 2D NMR techniques: ^{1}H–^{1}H COSY, ^{13}C–^{1}H HMQC, and ^{13}C–^{1}H HMBC. These experiments were performed using standard Bruker microprograms. Low-resolution and high-resolution electron impact mass spectra (EIMS) were measured using a Finnigan MAT95XP double-focusing mass spectrometer. Low-resolution electrospray ionization mass spectra (ESIMS) were recorded using Waters Quattro Micro™ API, and high-resolution mass spectra (HRMS) were obtained using an Agilent 6210 Time-of-Flight LC–MS system. Flash column chromatography was conducted manually using Merck silica gel 60 (35–70 μm) with an overpressure of 200 mbars. Amination reactions using 33% aqueous ammonia were carried out using a high-pressure reactor. Elemental analysis was performed using a EuroEA3000 series CHNS analyzer.

Compounds **B1**,[22] **B2**,[23] and **D12**[24] were synthesized following literature procedures, while **B4** is commercially available. Detailed procedures and characterization data for all other compounds are provided in the Supporting Information.

Biology

In vitro evaluation of DzNep analogues

Induction of apoptosis in HCT116 cells: p53 Knock out (KO) HCT116 cells that express inducible E2F1 (ER–E2F1) were used to assess the ability of DzNep analogues to induce E2F1-dependent apoptosis.[14] To activate E2F1, 4-hydroxytamoxifen (4-OHT) (300 nM) was added to the tissue culture medium. Cell apoptosis induced by DzNep analogues was measured in the presence or absence of 4-OHT for

72 h by analysis of DNA content via FACS. To measure the ability of DzNep analogues to synergize with a histone deacetylase inhibitor (HDACi) for apoptosis induction, DLD1 cells were treated with DzNep analogues (5 μM) for 48 h followed by HDACi trichostatin A (TSA) (150 nM) for an additional 24 h before being harvested for FACS analysis. To assess the apoptosis induction, cells were harvested and fixed in 70% ethanol. Fixed cells were stained with propidium iodide (50 $\mu g\,mL^{-1}$) after treatment with RNase (100 $\mu g\,mL^{-1}$). The FACS analysis of stained cells was done in FACScalibur flow cytometer (Becton Dickinson Instrument, San Jose, CA, USA). Cell cycle fractions were quantified using the CellQuest software (Becton Dickinson). Apoptosis was determined by measuring the DNA content of cells in sub-G1.

Production and purification of recombinant SAHH: The glutatione *S*-transferase (GST)-tagged SAHH in the pDEST 565 vector was expressed in *Escherichia coli* BL21 (DE3) pLysS and inoculated overnight in LB medium with chloramphenicol (34 $\mu g\,mL^{-1}$) and ampicillin (100 $\mu g\,mL^{-1}$) at 37 °C with orbital shaking at 200 rpm. The culture was then diluted 1:250 in LB medium with chloramphenicol and ampicillin, and maintained at 30 °C until the OD_{600} value reached 0.5–0.6 arbitrary units. After the addition of isopropyl-β-D-1-thiogalactopyranoside (400 μM), the culture was incubated for an additional 16 h and centrifuged at 6000 rpm for 40 min. at 4 °C. The bacterial pellet was then collected by centrifugation and lysed by sonication in buffer containing $Na_3(PO_4)$ (10 mM), NaCl (150 mM), DNAseI (5 $\mu g\,mL^{-1}$), lysozyme (0.625 $mg\,mL^{-1}$), 1X protease inhibitor (pH 7.4), and 2-mercaptoethanol (5 mM). The overexpressed protein was purified using the Bio-Scale Mini Profinity GST 5 mL cartridges (BioRad) followed by concentration and desalting in Tris buffer (2 mM, pH 8.0) with NaCl (100 mM). The concentrated SAHH–GST was cleaved with Tobacco Etch Virus (TEV) protease at 1 μg TEV per 50 μg GST-tagged protein in Tris buffer (100 mM, pH 8.0) with NaCl (100 mM), and dithiothreitol (DTT) buffer (2 mM). The cleaved GST was removed using glutathione Sepharose 4B beads (GE Healthcare) after 1 h incubation in Tris buffer (10 mM, pH 7.5) with NaCl (50 mM).

SAHH activity assay: The thiol-containing products of the SAHH-catalyzed reaction were detected in a 96-well format through the florescent thiol detection reagent, ThioGlo1 (Calbiochem). Freshly prepared SAHH (5 μL; 100 $ng\,\mu L^{-1}$ in 100 mM Tris pH 7.5) was added to inhibitor/DMSO control (5 μL) and freshly prepared assay buffer (15 μL; 100 mM Tris pH 7.5 with 3 μM DTT, 150 μM NAD, and 3 mM EDTA) and incubated at 37 °C for 30 min. After incubation, SAHH (Sigma, 5 μL of 750 μM, freshly prepared in 100 mM Tris, pH 7.5) was added and further incubated at 37 °C for 10 min. 500 μM. ThioGlo1 freshly diluted in Tris buffer (100 mM, pH 7.5) was added and incubated at 37 °C for another 15 min. The fluorescence signal was detected by Safire2 (Tecan) with a 380 nM excitation and 510 nM emission filter. IC_{50} measurements were performed using GraphPad Prism version 5.00 for Windows (GraphPad software, San Diego, CA, USA).

In vivo antitumor assessment of DzNep analogues

All animal studies were conducted in compliance with animal protocols approved by the A*STAR–Biopolis Institutional Animal Care and Use Committee (IACUC) of Singapore.

The female athymice BALB/c nude mice (5–8 week-old) were housed in the Biological Resource Centre. Mice were implanted subcutaneously in flank with 5×10^6 cells of HCT116 parental human colon carcinoma. When tumors reached $\approx$200 mm^3, the mice were divided into four groups (10 mice per group) and were treated with vehicle or DzNep analogue **D9** at 30 and 80 $mg\,kg^{-1}$ by intraperitoneal (IP) injection for 14 days. Tumor growth and the whole body weight changes of mice were monitored every other day.

Student's t-test is used to determine the statistical significance of tumor volumes and body weight changes between groups. Statistical analyses are conducted at a p level of 0.05. SPSS was used for all statistical analyses and graphic presentations.

Acknowledgements

*The authors thank the Agency for Science, Technology and Research (A*STAR), Singapore (CCOG01-001-2008 and ETPL/10-FS0002) for financial support of this project.*

Keywords: deazaneplanocin A · epigenetics · neplanocin A · *S*-adenosylhomocysteine hydrolase (SAHH) · structure–activity relationships

[1] K. Helin, D. Dhanak, *Nature* **2013**, *502*, 480–488.
[2] a) J. S. Garcia, N. Jain, L. A. Godley, *Onco. Targets Ther.* **2010**, *3*, 1–13; b) O. A. O'Connor, M. L. Heaney, L. Schwartz, S. Richardson, R. Willim, B. MacGregor-Cortelli, T. Curly, C. Moskowitz, C. Portlock, S. Horwitz, A. D. Zelenetz, S. Frankel, V. Richon, P. Marks, W. K. Kelly, *J. Clin. Oncol.* **2006**, *24*, 166–173; c) R. L. Piekarz, R. Frye, M. Turner, J. J. Wright, S. L. Allen, M. H. Kirschbaum, J. Zain, H. M. Prince, J. P. Leonard, L. J. Geskin, C. Reeder, D. Joske, W. D. Figg, E. R. Gardner, S. M. Steinberg, E. S. Jaffe, M. Stetler-Stevenson, S. Lade, A. T. Fojo, S. E. Bates, *J. Clin. Oncol.* **2009**, *27*, 5410–5417.
[3] a) F. Crea, L. Fornaro, G. Bocci, L. Sun, W. L. Farrar, A. Falcone, R. Danesi, *Cancer Metastasis Rev.* **2012**, *31*, 753–761; b) F. Crea, E. M. Hurt, L. A. Mathews, S. M. Cabarcas, L. Sun, V. E. Marquez, R. Danesi, W. L. Farrar, *Mol. Cancer* **2011**, *10*, 40; c) J. A. Simon, C. A. Lange, *Mutat. Res.* **2008**, *647*, 21–29.
[4] J. Tan, X. Yang, L. Zhuang, X. Jiang, W. Chen, P. L. Lee, R. K. Karuturi, P. B. Tan, E. T. Liu, Q. Yu, *Genes Dev.* **2007**, *21*, 1050–1063.
[5] a) T. Chiba, E. Suzuki, M. Negishi, A. Saraya, S. Miyagi, T. Konuma, S. Tanaka, M. Tada, F. Kanai, F. Imazeki, A. Iwama, O. Yokosuka, *Int. J. Cancer* **2012**, *130*, 2557–2567; b) A. Hayden, P. W. Johnson, G. Packham, S. J. Crabb, *Breast Cancer Res. Treat.* **2011**, *127*, 109–119; c) J. K. Lee, K. C. Kim, *Biochem. Biophys. Res. Commun.* **2013**, *438*, 647–652; d) J. Zhou, C. Bi, L. L. Cheong, S. Mahara, S. C. Liu, K. G. Tay, T. L. Koh, Q. Yu, W. J. Chng, *Blood* **2011**, *118*, 2830–2839.
[6] S. K. Knutson, T. J. Wigle, N. M. Warholic, C. J. Sneeringer, C. J. Allain, C. R. Klaus, J. D. Sacks, A. Raimondi, C. R. Majer, J. Song, M. P. Scott, L. Jin, J. J. Smith, E. J. Olhava, R. Chesworth, M. P. Moyer, V. M. Richon, R. A. Copeland, H. Keilhack, R. M. Pollock, K. W. Kuntz, *Nat. Chem. Biol.* **2012**, *8*, 890–896.
[7] M. T. McCabe, H. M. Ott, G. Ganji, S. Korenchuk, C. Thompson, G. S. VanAller, Y. Liu, A. P. Graves, A. Della Pietra III, E. Diaz, L. V. LaFrance, M. Mellinger, C. Duquenne, X. Tian, R. G. Kruger, C. F. McHugh, M. Brandt, W. H. Miller, D. Dhanak, S. K. Verma, P. J. Tummino, C. L. Creasy, *Nature* **2012**, *492*, 108–112.
[8] W. Qi, H. Chan, L. Teng, L. Li, S. Chuai, R. Zhang, J. Zeng, M. Li, H. Fan, Y. Lin, J. Gu, O. Ardayfio, J. H. Zhang, X. Yan, J. Fang, Y. Mi, M. Zhang, T. Zhou, G. Feng, Z. Chen, G. Li, T. Yang, K. Zhao, X. Liu, Z. Yu, C. X. Lu, P. Atadja, E. Li, *Proc. Natl. Acad. Sci. USA* **2012**, *109*, 21360–21365.
[9] Z. N. Wee, Z. Li, P. L. Lee, S. T. Lee, Y. P. Lim, Q. Yu, *Cell Rep.* **2014**, *8*, 204–216.
[10] W. Kim, G. H. Bird, T. Neff, G. Guo, M. A. Kerenyi, L. D. Walensky, S. H. Orkin, *Nat. Chem. Biol.* **2013**, *9*, 643–650.
[11] a) J. H. Cho, D. L. Bernard, R. W. Sidwell, E. R. Kern, C. K. Chu, *J. Med. Chem.* **2006**, *49*, 1140–1148; b) B. Y. Michel, P. Strazewski, *Tetrahedron* **2007**, *63*, 9836–9841.
[12] H. Osato, I. L. Jones, A. Chen, C. L. L. Chai, *Org. Lett.* **2010**, *12*, 60–63.

[13] X. Jiang, J. Tan, J. Li, S. Kivimae, X. Yang, L. Zhuang, P. L. Lee, M. T. Chan, L. W. Stanton, E. T. Liu, B. N. Cheyette, Q. Yu, *Cancer Cell* **2008**, *13*, 529 – 541.
[14] Y. Zhao, J. Tan, L. Zhuang, X. Jiang, E. T. Liu, Q. Yu, *Proc. Natl. Acad. Sci. USA* **2005**, *102*, 16090 – 16095.
[15] M. A. Turner, X. D. Yang, D. Yin, K. Kuczera, R. T. Borchardt, P. L. Howell, *Cell Biochem. Biophys.* **2000**, *33*, 101 – 125.
[16] a) P. K. Chiang, *Pharmacol. Ther.* **1998**, *77*, 115 – 134; b) E. De Clercq, *Nucleosides Nucleotides Nucleic Acids* **2005**, *24*, 1395 – 1415; c) C. K. Tseng, V. E. Marquez, R. W. Fuller, B. M. Goldstein, D. R. Haines, H. McPherson, J. L. Parsons, W. M. Shannon, G. Arnett, M. Hollingshead, J. S. Driscoll, *J. Med. Chem.* **1989**, *32*, 1442 – 1446.
[17] M. S. Wolfe, R. T. Borchardt, *J. Med. Chem.* **1991**, *34*, 1521 – 1530.
[18] M. Bray, J. Driscoll, J. W. Huggins, *Antiviral Res.* **2000**, *45*, 135 – 147.
[19] S. Shuto, T. Obara, M. Toriya, M. Hosoya, R. Snoeck, G. Andrei, J. Balzarini, E. De Clercq, *J. Med. Chem.* **1992**, *35*, 324 – 331.
[20] H. O. Kim, S. J. Yoo, H. S. Ahn, W. J. Choi, H. R. Moon, K. M. Lee, M. W. Chun, L. S. Jeong, *Bioorg. Med. Chem. Lett.* **2004**, *14*, 2091 – 2093.
[21] a) L. L. Bennett, Jr., B. J. Bowdon, P. W. Allan, L. M. Rose, *Biochem. Pharmacol.* **1986**, *35*, 4106 – 4109; b) M. Hasobe, J. G. McKee, D. R. Borcherding, B. T. Keller, R. T. Borchardt, *Mol. Pharmacol.* **1988**, *33*, 713 – 720.
[22] K. Fukukawa, T. Ueda, T. Hirano, *Chem. Pharm. Bull.* **1983**, *31*, 1842 – 1847.
[23] Y. X. Tan, S. Santhanakrishnan, H. Y. Yang, C. L. L. Chai, E. K. W. Tam, *J. Org. Chem.* **2014**, *79*, 8059 – 8066.
[24] S. M. Siddiqi, X. Chen, S. W. Schneller, S. Ikeda, R. Snoeck, G. Andrei, J. Balzarini, E. De Clercq, *J. Med. Chem.* **1994**, *37*, 1382 – 1384.
[25] R. K. Gordon, K. Ginalski, W. R. Rudnicki, L. Rychlewski, M. C. Pankaskie, J. M. Bujnicki, P. K. Chiang, *Eur. J. Biochem.* **2003**, *270*, 3507 – 3517.
[26] L. S. Jeong, S. J. Yoo, K. M. Lee, M. J. Koo, W. J. Choi, H. O. Kim, H. R. Moon, M. Y. Lee, J. G. Park, S. K. Lee„ M. W. Chun, *J. Med. Chem.* **2003**, *46*, 201 – 203.
[27] R. Snoeck, G. Andrei, J. Neyts, D. Schols, M. Cools, J. Balzarini, E. De Clercq, *Antiviral Res.* **1993**, *21*, 197 – 216.
[28] Y. Kitade, T. Ando, T. Yamaguchi, A. Hori, M. Nakanishia, Y. Ueno, *Bioorg. Med. Chem.* **2006**, *14*, 5578 – 5583.

Received: July 26, 2014
Published online on ■■ ■■, 0000

Epigenetic agents against cancer: 3-Deazaneplanocin A and neplanocin A are known to reactivate tumor suppressors leading to apoptosis in cancer cells; however, their exact mode of action is not fully understood. Here, 42 analogues were evaluated in cell- and enzyme-based assays. No direct correlation between cytotoxicity and SAHH inhibitory activity was found. The SAR studies identified two compounds with good PK and safety profiles that warrant closer investigation.

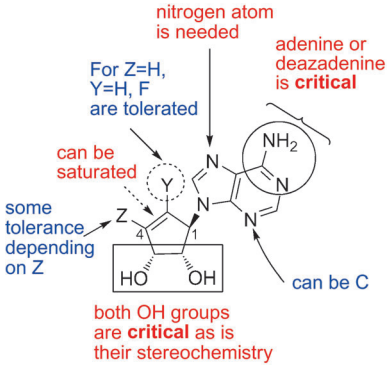

E. K. W. Tam, T. M. Nguyen, C. Z. H. Lim, P. L. Lee, Z. Li, X. Jiang, S. Santhanakrishnan, T. W. Tan, Y. L. Goh, S. Y. Wong, H. Yang, E. H. Q. Ong, J. Hill, Q. Yu, C. L. L. Chai**

■■ – ■■

3-Deazaneplanocin A and Neplanocin A Analogues and Their Effects on Apoptotic Cell Death